



Analysis of Electrical Measurements on Cadmium Chloride Doped PVA-PVP Blend

Basavarajeshwari M Baraker* and Blaise Lobo †

Abstract

Films of Polyvinylalcohol (PVA) - Polyvinylpyrrolidone (PVP) blend, doped with cadmium chloride (CdCl_2) from 0.5 wt% up to 40 wt% and prepared by solution casting method, were studied using temperature dependent direct current (DC) electrical measurements. The DC electrical data were analyzed using Variable Range Hopping (VRH) model in the temperature range varying from 303 K up to 318 K. The Mott parameters were determined. The study of time evolution of current passing through the sample, when a step voltage is applied across it reveals that ions are the majority charge carriers, but the role of electrons in charge transport cannot be neglected. The activation energy (E_a) for mobility of charge carriers has been calculated from VRH and Arrhenius models.

Keywords: Electrical conductivity; VRH model; Cadmium Chloride; PVA-PVP blend; Arrhenius relation.

PACS: 72.80.Le, 73.63.Bd, 81.05.Lg

* Karnatak University's Karnatak Science College, Dharwad, Karnataka, India; brajeshwari31@gmail.com

† Karnatak University's Karnatak Science College, Dharwad, Karnataka, India; blaise.lobo@gmail.com

1. Introduction

The study of solid polymeric electrolytes and polymeric blends has assumed importance in recent times, due to improvement in properties of the resulting material and their potential applications in devices like batteries, fuel cells and super-capacitors [1-3]. The study of nano-structured polymeric blends is a matter of contemporary research interest, due to the range of options available to tailor a material, in order to suit particular needs [4]. Metal nano-particles encapsulated by polymeric molecules show interesting optical properties, suitable for various applications [5, 6]. Polyvinylalcohol (PVA) is a polymeric material which has drawn the attention of several researchers due to its multifunctionality [7] and useful properties such as hydrophilic nature, biodegradability, biocompatibility [8] and good processability on film formation. PVA doped with different red-ox agents like iodine/ potassium iodide [9], titanium chloride [10], barium chloride [11], potassium nitrate- magnesium chloride [12], sodium iodide [13] and other inorganic salts have been studied. Polyvinylpyrrolidone (PVP) has good water absorption and complex forming abilities [14]. Doped PVP has also been studied [15]. Both PVA and PVP are water soluble in nature [16, 17]. When a polymeric blend is doped; the dopant can produce modifications in molecular structure of the material. Hence, changes in the microstructural features and physical properties of polymeric material are observed. These micro-structural modifications depend on nature of dopant and ways in which the dopant chemical species may interact with polymer molecules of the host material [18]. Several researchers have studied the structure and properties of doped polymeric blends and nano-structured polymeric systems [19-28].

When PVA-PVP blend is doped with CdCl_2 , significant changes in microstructure of the polymeric host takes place. The details of Scanning Electron Microscope (SEM) and Atomic Force Microscope (AFM) studies on CdCl_2 doped PVA-PVP blend have been elaborated by us elsewhere [26, 27]. The SEM micrographs of pure PVA-PVP blend, when compared to that of CdCl_2 doped PVA-PVP blend films reveal significant morphological variations, which indicate that there are chemical interactions between the dopant

species (that is, Cadmium, Cd^{2+} , and Chlorine, Cl^- , ions) with the polymer molecules. This interpretation is supported by spectroscopic investigations on CdCl_2 doped PVA-PVP blend films, details of which have been published by us earlier [26]. The discussion of electrical parameters requires an understanding of microstructural changes which occur in the PVA-PVP blend sample, on doping with CdCl_2 . SEM micrographs confirm formation of dopant nano-structures (nano-spheres, nano-rods and nano sized flower shaped structures), aggregation of dopant species (meso-scale structures and micro-structural globular features of dopant) and finally, percolation effect (uniform morphology), at increasing levels of CdCl_2 doping in PVA-PVP blend films. At 0.0 wt% of dopant, miscibility of PVA and PVP components are confirmed by a uniform and homogeneous surface. At 0.5 wt% of CdCl_2 in PVA-PVP blend, there is formation of nano-structures (spheres) of average diameter 260.8 ± 10.7 nm which are uniformly distributed throughout the sample. The linear dimension of these nano-particles is in the range varying from 130.4 nm up to 347.8 nm. As the dopant level increases to 2.2 wt%, there are self-grown nano-rods of average length $2.4 \pm 0.1 \mu\text{m}$ (diameter 170.2 ± 1.9 nm). These nano-rods are uniformly distributed throughout the sample. Along with nano-rods, there are white patches in the SEM micrographs, which reveal the multi-crystalline regions of dopant in the blend sample at 2.2 wt% doping level. At the dopant level of 3.3 wt%, complex networks of nano-clusters having average dimension 431.1 ± 19.2 nm are seen in the SEM micrographs. At 10.2 wt% dopant level, three dimensional structures (globules) of linear dimension (diameter) varying from $1.67 \mu\text{m}$ up to $6.33 \mu\text{m}$ (corresponding to an average dimension $4.00 \pm 0.15 \mu\text{m}$) are formed. The formation of nano-crystalline and micro-crystalline regions in the polymeric material (doped from 0.5 wt% up to 10.2 wt%) is supported by the XRD scans. At 12.1 wt% doping level, three dimensional micro-globules get degraded in the host PVA-PVP blend. In the higher dopant region, from 15.5 wt% up to 40.0 wt%, a homogeneous, smooth surface in SEM micrographs indicate the uniform distribution of dopant in the polymer matrix, due to percolation effect. At these higher levels of doping, the SEM micrographs [26, 27] reveal a homogeneous surface, implying a

completely amorphous nature of the doped film, a conclusion which is supported by the XRD scans.

The analysis of electrical and SEM data is supported by XRD measurements (See Figure 1(a) and Figure 1(b)). The details of study on CdCl_2 doped blend films using XRD technique has already been published [27]. A review of the same and some additional details are presented here, in order to aid the study of electrical data on these films. X-ray diffraction patterns were obtained using Cu K_α radiation of wavelength 1.5406 \AA , for diffraction angle (2θ) varying from 10° up to 80° .

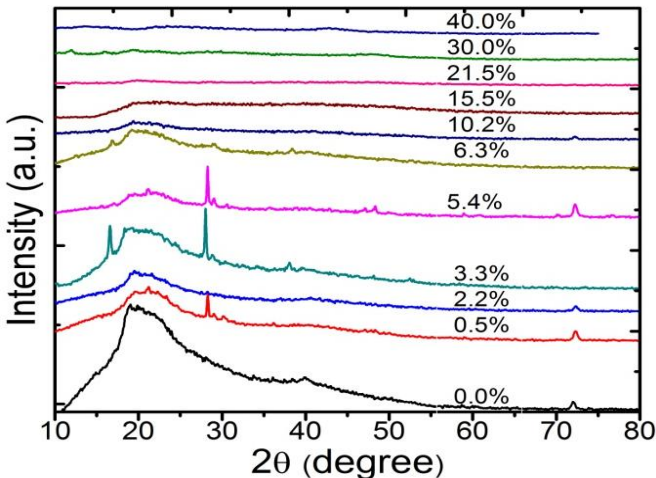


Figure 1(a) XRD scans of CdCl_2 doped PVA-PVP blend films, from doping level 0.0 wt% up to 40.0 wt%.

The XRD scans show a broad diffraction peak (halo) at $2\theta=20^\circ$, which reveals semi-crystalline nature of the film. This corresponds to (110) reflections (JCPD file No. 41-1049). The presence of more than one diffraction peak reflects the existence of multi-crystallite regions in the doped blends. During interactions between functional groups of PVA, PVP and dopant ions (Cd^{2+} and Cl^-), displacement of atoms from their lattice sites produces dislocations, and hence, the broadening of the diffracted peaks is observed. An increase in peak intensity is observed for films doped with CdCl_2 , from 0.5 wt% up to 3.3 wt%, which indicates that there is increase in degree of crystallinity of the doped films at these low levels of doping. In case of films with doping levels varying from 5.4 wt%

up to 40.0 wt%, decreased intensity of this crystalline peak suggests enhancement in amorphousness of CdCl_2 doped PVA-PVP blend films [29]. The decrease in XRD peak intensity and increase in full width at half maximum (FWHM) of the crystallite peaks are due to inter-molecular interaction between solvent (H_2O) and polymer blend [30-32]. The nature of crystalline peaks also suggest a possibility of conformational transformation between different crystalline phases of dopant species, in the doping levels ranging from 0.5 wt% up to 5.4 wt % (See Figure 1(b)).

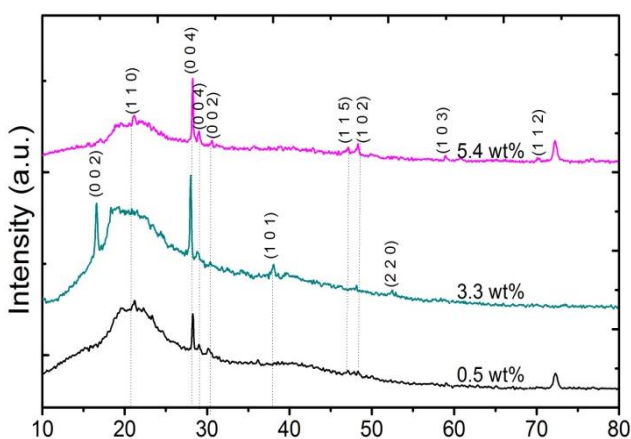


Figure 1(b). XRD scans of semi-crystalline CdCl_2 doped PVA-PVP blend films, for doping levels 0.5 wt%, 3.3 wt% and 5.4 wt%, with indexing.

In Figure 1(a), the existence of a broad diffraction peak at about $2\theta=20^\circ$ confirms the semi-crystalline nature of PVA, and it corresponds to (110) reflections (JCPDS file No. 41-1049). For cadmium chloride monohydrate ($\text{CdCl}_2 \cdot \text{H}_2\text{O}$) with orthorhombic structure, $a=9.520\text{\AA}$, $b=3.776\text{\AA}$, $c=11.890\text{\AA}$ and angles; $\alpha=\beta=\gamma=90^\circ$; with reference to JCPDS file No.00-001-0161, the intense peaks in $\text{CdCl}_2 \cdot \text{H}_2\text{O}$ have Miller indices (1 0 1), (0 0 2), (2 0 0), (1 0 3), (0 0 4), (3 1 1) and (5 0 1), and attributed to the crystalline peaks at diffraction angle, $2\theta = 12.39^\circ$, 15.34° , 19.35° , 24.72° , 30.16° , 37.25° and 48.9° , respectively [33]. On addition of CdCl_2 into PVA-PVP blend, additional sharp peaks appear in XRD scans of samples doped from 0.5 wt% up to 5.4 wt%, at $2\theta = 23.6^\circ$, 28.3° , 29.1° , 30.6° , 36.2° , 38.1° , 43.5° , 47.1° , 48° and 70.1° , which clearly evidences the presence of CdCl_2 and cadmium (Cd) metal nano-structures of various sizes

in the PVA-PVP matrix. Indexing the sharp peaks of CdCl_2 doped PVA-PVP blend films has been done with reference to JCPDS file number 00-001-0007 for cadmium metal with hexagonal structure, $a=b=2.9793\text{\AA}$, $c=5.6181\text{\AA}$, and angles $\alpha=\beta=90^\circ$ and $\gamma=120^\circ$ [34].

2. Experimental Details

2.1 Materials

The procedure for preparation of CdCl_2 doped PVA-PVP blend films has been described by us elsewhere [24, 27]. However, for the sake of completeness, a brief report on the same is given here. Semicrystalline PVA (1,40,000 molecular weight) and amorphous PVP (50,000 molecular weight) were purchased from HiMedia Laboratories Pvt. Ltd, Mumbai. CdCl_2 doped PVA-PVP blend films are prepared by solution casting method. Aqueous solution of blend samples were prepared by taking PVA and PVP in ratio of 50:50 (proportion by weight) and dissolving in double distilled water, by stirring the mixture for 24 hours using a magnetic stirrer. A standard solution of dopant is prepared by dissolving cadmium chloride monohydrate ($\text{CdCl}_2\cdot\text{H}_2\text{O}$) in double distilled water. Different volumes of the standard dopant solution were added to aqueous solutions of PVA-PVP blends, to get CdCl_2 doped blend samples, with doping level varying from 0.5 wt% up to 40 wt%. After drying, doped films were peeled off from the glass substrate, carefully labeled and stored. An air cooled, temperature controlled oven maintained at 40°C was used to dry the samples. The procedure of preparation of these films is illustrated in Figure 2. The films prepared were characterized using optical spectroscopy [25], AFM, SEM, Differential Scanning Calorimetry (DSC), electrical measurements [24, 27], FTIR, FT-Raman, UV-Vis, EDS and Fluorescence Spectrometry [26]. In this paper, the detailed analysis of DC electrical measurements is described. The electrical properties of polymer films also depend on dopant concentration [35, 36].

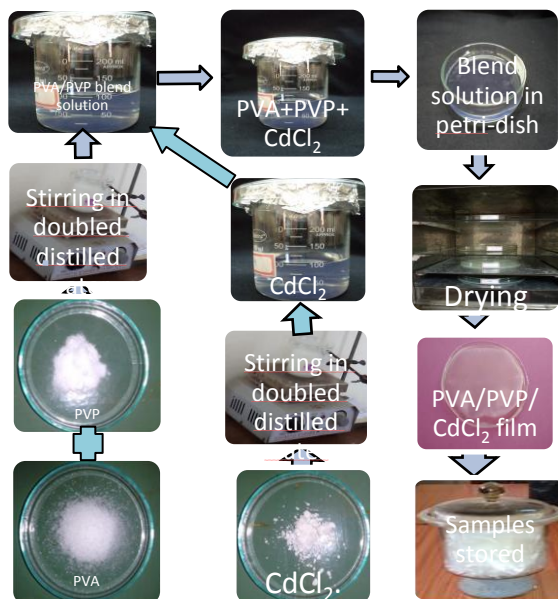


Figure 2 Pictorial illustration regarding the preparation of CdCl₂ doped PVA-PVP blend films, using solution casting method. The pictures are self-explanatory, and can also be understood with help of the text (sample preparation procedure), which is elaborated in section 2.1 of this paper.

2.2 Methods

A 'two probe' technique was employed for measuring the temperature dependence of electrical conductivity of CdCl₂ doped PVA-PVP blend films. An electrical set-up (with research quality equipment) comprising two probe set up with a digital picoammeter (model: DPM-111), high voltage supply (model: EHT-11) and temperature variation apparatus with PID controlled oven (model: PID-200) from SES instruments Private Limited, Roorkee, Uttarakhand (UK), India have been used. Transference number measurements were performed from the observation of time evolution of DC electric current, keeping silver electrode on one side of the sample, and using graphite electrode as the blocking electrode on the other side.

3. Results and Discussion

The measurement of temperature dependence of electrical conductivity of doped polymeric materials gives an idea about nature of charge transport in them. In this paper, the plot of

activation energy (E_a) determined using the Arrhenius relation (E_a versus doping level of CdCl_2 in PVA-PVP blend) is shown in figure 3. The plot of average activation energy ($\langle E_a \rangle$) determined using the VRH model, versus doping level of CdCl_2 in PVA-PVP blend, is shown in figure 4. The prepared (solution cast) un-doped and doped PVA-PVP films were characterized by measuring the electrical conductivity at different temperatures. The activation energy was first determined using Arrhenius equation (using equation 1).

$$\sigma = \sigma_0 \exp\left(\frac{-E_a}{k_B T}\right) \quad (1)$$

In equation (1), σ is electrical conductivity, σ_0 is pre-exponential factor; the projected electrical conductivity at infinite temperature, E_a is activation energy at temperature T and k_B is Boltzmann constant. The variation of activation energy for CdCl_2 doped PVA-PVP blends, doped from 0.5 wt% up to 40 wt% have been studied in the temperature range 303 K - 318 K. The data (see figure 3(a)) clearly shows three different regions, which have been attributed to formation of nano-structures, aggregation of dopant species and percolation of dopant, respectively [27]; this interpretation is supported by SEM and XRD studies, details of which have been discussed in the introductory section of this paper. At lower dopant concentrations (from 0.5 wt% up to 3.3 wt %), there is an increase in activation energy from 1.60 eV to 1.82 eV, implying a decrease in electrical conductivity. Increase in E_a of the sample on addition of CdCl_2 in the blend (decrease in electrical conductivity, see figure 3b) is due to creation of blockages in conducting pathway due to the formation of nano structures, as seen in the SEM images [26, 27].

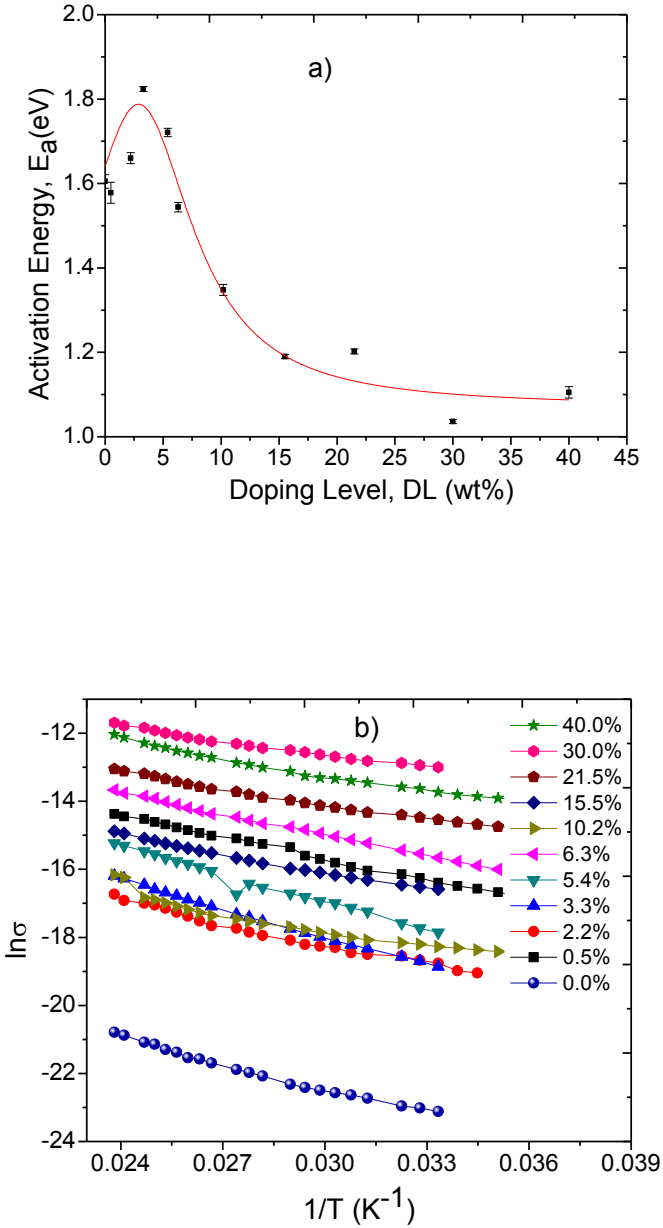


Figure 3 (a) Variation of activation energy (E_a) with respect to the doping level of CdCl₂ in PVA-PVP blend, determined using Arrhenius relation. (b) $\ln \sigma$ versus $1/T$ at different concentrations of CdCl₂.

The obstruction in movement of mobile ions by nano-structures in the polymeric blend material leads to reduction in ion and segmental mobility through the polymer matrix [27]. Consequently, a drop in electrical conductivity of the sample and an increase in activation energy for mobility of charge carriers are observed. On increasing the concentration of CdCl₂ in PVA-PVP blend further, from 3.3 wt% up to 15.5 wt%, a decrease in activation energy (see figure 3(a)), from 1.82 eV down to 1.19 eV is observed. At the doping levels ranging from 5.4 wt% up to 10.2 wt%, SEM micrographs [26, 27] show increased aggregation of dopant nano-structures to form meso- and micro- scale structures in the polymeric host. The polymeric molecules acts as insulating barrier between conducting regions, across which hopping of charge carriers take place. This causes the reduction in crystalline-amorphous interface, decreasing the interfacial barrier and increasing the transition probability of (charge carriers) hopping across barrier and insulator chain, which provides the conducting path for mobile charge carriers through the amorphous region of the polymer matrix and consequently, an enhancement of electrical conductivity of the doped polymeric material [37, 38]. At higher dopant concentrations, in the doping range varying from 15.5 wt% up to 40.0 wt%, the activation energy is almost constant (1.2 eV; refer Table 1). So, a percolation threshold is reached at 15.5 wt%. Due to percolation effect [39], the dopant is evenly distributed throughout the polymer matrix and forms an amorphous material with a homogeneous surface. Hence, increased electrical conductivity is observed at higher concentrations (from 15.5 wt% up to 40.0 wt%) of CdCl₂ in PVA-PVP blend films. The higher segmental mobility, and hence, the increased movement of ions through the polymer matrix leads to this increase in electrical conductivity.

The increase in DC conductivity of the doped polymeric blend, as a function of temperature is due to thermally stimulated free movement of mobile charge carriers. An increase in temperature of the doped polymeric film results in increased free volume and greater segmental mobility of polymer chains, thereby increasing the electrical conductivity [40]. Disorder arises due to semi-crystallinity (existence of crystalline amorphous interfaces and amorphous regions), impurities and the lack of long range order

[41]. SEM, XRD and DSC scans, details about which have been published earlier [26, 27], reveal formation of nano-crystalline and micro-crystalline regions due to dopant in the host polymeric blend, in the doping range varying from 0.5 wt% up to 10.2 wt%. For localized charge carriers, charge transport takes place via phonon-assisted hopping between localized sites. Due to the localized states introduced by doping PVA-PVP blend with CdCl_2 , charge transport may be between nearest neighbor sites [42]. The Variable Range Hopping (VRH) model is obeyed for three dimensional hopping of charge carriers, as revealed by the temperature ($T^{-1/4}$) dependence of electrical conductivity (see Figure 4(b) and equation 2). Three dimensional Variable range hopping model (according to Mott-Davis [43, 44]) is feasible, as the measured temperature variation of electrical conductivity data gives a good fit (on comparison) with equation (2), taking the value of γ to be 0.25 (which corresponds to three dimensional VRH).

$$\sigma T^{\frac{1}{2}} = \sigma_0 \exp \left\{ - \left[\frac{T_0}{T} \right]^\gamma \right\} \quad (2)$$

In equation (2), σ is the DC electrical conductivity, T is temperature (K), σ_0 ($\text{Sm}^{-1}\text{K}^{1/2}$) is the pre-exponential factor [44], T_0 is characteristic temperature, and $\gamma = \frac{1}{D+1}$ (where D is the dimension). Note that, in equation (2), the value of γ is 1/4, 1/3 and 1/2 for 3D, 2D and 1D variable range hopping of charge carriers, respectively.

$$\sigma_0 = \left(\frac{A^2 N(E_F)}{\alpha} \right)^{\frac{1}{2}} \quad (3)$$

In equation (3), $N(E_F)$ is density of states ($\text{eV}^{-1}\text{m}^{-3}$), α is wave function decay constant (m^{-1}) and A is complex parameter [45, 46]. σ_0 is expressed in $\text{Sm}^{-1}\text{K}^{1/2}$.

$$A = \left(\frac{3e^2 \nu_{ph}}{\sqrt{8\pi k_B}} \right) \quad (4)$$

In equation (4), e is charge of an electron (1.602×10^{-19} C), ν_{ph} is phonon frequency (10^{13} Hz) and k_B is the Boltzmann constant (8.615×10^{-5} eVK $^{-1}$).

The complex parameter 'A' is expressed in $\text{C}^2\text{s}^{-1}\text{eV}^{-1/2}\text{K}^{1/2}$.

The characteristic temperature (T_0) is calculated using equation (5).

$$T_0 = \frac{16\alpha^3}{kN(E_F)} \quad (5)$$

In equation (5), T_0 is expressed in kelvin (K). In the present work, for temperature range varying from 303 K up to 318 K, the activation energy (E_a) has been calculated for CdCl₂ doped PVA-PVP samples, using relation (6).

$$E_a = \gamma k_B T_0 \left(\frac{T_0}{T} \right)^{\gamma-1} \quad (6)$$

The activation energy (E_a) is expressed in units of electron volt (eV), and obtained using VRH model (see figure 4(a)) by substituting the value of T_0 in equation (6). A series of values (for E_a) is obtained at different absolute temperatures (T), and the average value, $\langle E_a \rangle$, is calculated. Table 1 lists the calculated data. Note that VRH model shows the same trend for variation of activation energy versus doping level, as that obtained from the Arrhenius model. The characteristic temperature, density of states, range of hopping and energy of hopping has been determined by assuming that the localization decay constant (α^{-1}) is 3 Å.

Variation of hopping energy (W_{hop}) with doping level of CdCl₂ in PVA-PVP blend (expressed in wt%) is shown in figure 5. Variation of range of hopping (R_{hop}) with doping level (expressed in wt%) of CdCl₂ in PVA-PVP blend is shown in figure 6. The value of W_{hop} is more at lower doping levels; hopping energy is more due to smaller size nano-structures and more separation (R_{hop}) between them (refer Table 2). Mobile charged particles need more potential energy to overcome the barrier at nano-structures and hence, the energy needed to overcome this potential is more. Energy needed to hop from one energy state to another is more for samples doped from 0.5 wt% up to 5.4 wt%, and hence, less electrical conductivity and more activation energy have been observed. For samples with doping levels 6.3 wt% and above, W_{hop} has smaller value, which is due to the change of sample structure from nano-scale to meso/micro-scale, thereby providing smaller separation (R_{hop}) between the available energy states. Hence, range of hopping is lesser than for lower doping levels, leading to the sample having more electrical conductivity. At higher doping levels; that is, at 15.5 wt% and above, due to increased amorphousness, the existence of

more number of Cd^{2+} and Cl^- ions and the existence of a larger number of conducting paths results in a smaller hopping range (distance), yielding a material with increased electrical conductivity.

Doping Level of CdCl_2 in PVA-PVP blend DL (wt%)	From Arrhenius Equation E_a (eV)	Parameters determined from Variable Range Hopping (VRH) Model Relation				
		$\langle E_a \rangle$ (eV)	T_0 ($\times 10^{11}\text{K}$)	$\langle W_{\text{hop}} \rangle$ (eV)	$\langle R_{\text{hop}} \rangle$ (nm)	$N(E_F)$ ($\times 10^{21}\text{e V}^{-1}\text{m}^{-3}$)
0.0	1.605 \pm 0.016	1.621 \pm 0.014	11.0	5.9	27.4	6.26
0.5	1.578 \pm 0.025	1.699 \pm 0.019	13.3	6.8	28.8	5.19
2.2	1.660 \pm 0.013	1.676 \pm 0.017	12.4	6.7	28.3	5.56
3.3	1.824 \pm 0.006	1.803 \pm 0.018	16.6	7.2	30.3	4.14
5.4	1.721 \pm 0.010	1.726 \pm 0.019	13.8	6.9	28.8	5.00
6.3	1.544 \pm 0.004	1.536 \pm 0.018	8.69	6.1	25.7	7.91
10.2	1.348 \pm 0.013	1.365 \pm 0.015	5.40	5.5	23.0	12.7
15.5	1.190 \pm 0.005	1.205 \pm 0.013	3.27	4.8	20.2	21.4
21.5	1.202 \pm 0.006	1.219 \pm 0.017	3.88	5.0	21.0	17.7
30.0	1.036 \pm 0.005	1.032 \pm 0.011	1.76	4.1	17.4	39.1
40.0	1.105 \pm 0.013	1.127 \pm 0.013	2.56	4.5	19.1	26.8

Table 1 Activation energies for charge carrier mobility extracted from experimental study of temperature dependence of DC electrical conductivity of PVA-PVP blend films, doped with different concentrations (doping levels) of CdCl_2 .

Transport or transference number is the fraction of current carried by a particular charge species (ions or electrons). In polymer solid electrolytes, the electrical conductivity is due to mobility of ions (cations and anions) and/or electrons. Various structural and non-structural parameters can affect the ionic conductivity. They include the arrangement of crystals, ion-ion interactions, degree of disorder, concentration of mobile ions, size of the ions, bonding characteristic, ionic polarizability, presence of conducting pathways, and existence of vibrational and rotational motion of ions.

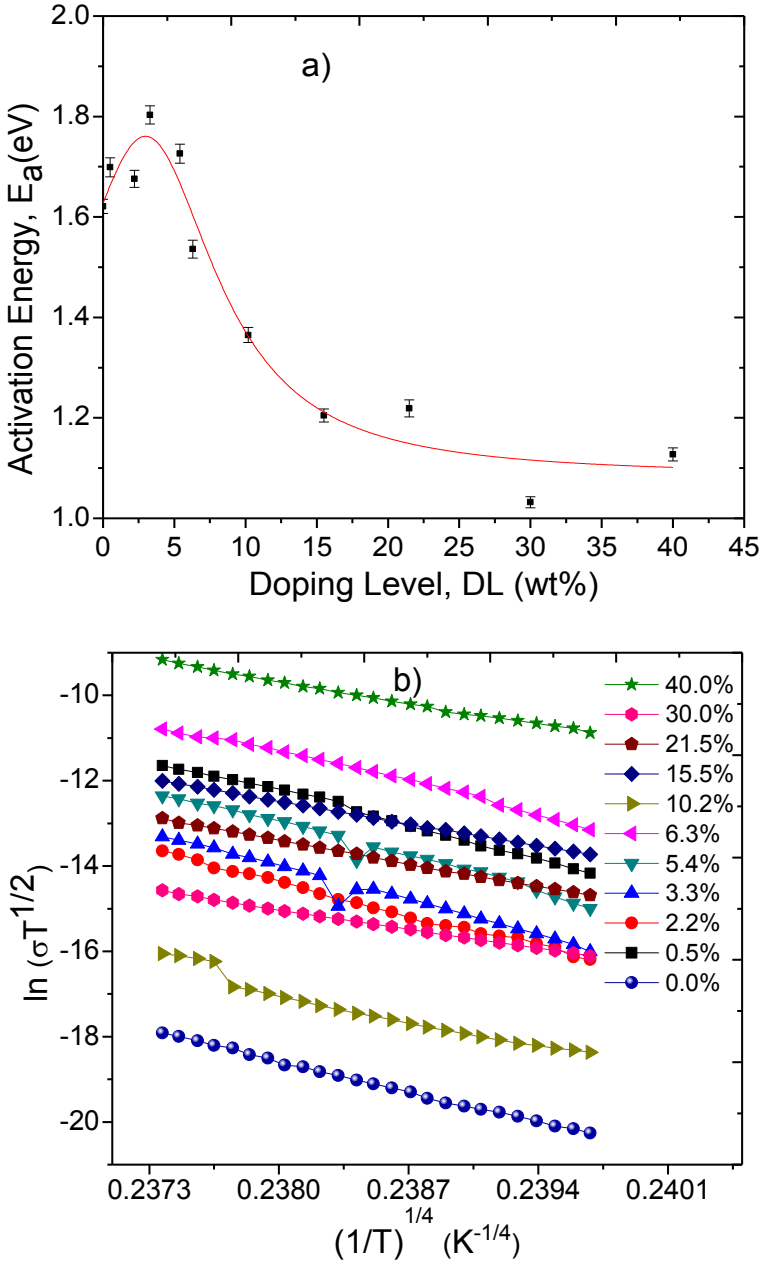


Figure 4 (a) Variation of average activation energy ($\langle E_a \rangle$) determined using VRH model with respect to the doping level of CdCl₂ in PVA-PVP blend. (b) The plot of $\ln(\sigma T^{1/2})$ versus $\frac{1}{T^{1/4}}$ shows good linear fit, implying Variable Range Hopping (VRH) in three dimensions is a good model for interpretation of results of DC electrical conductivity in CdCl₂ doped PVA-PVP blend films.

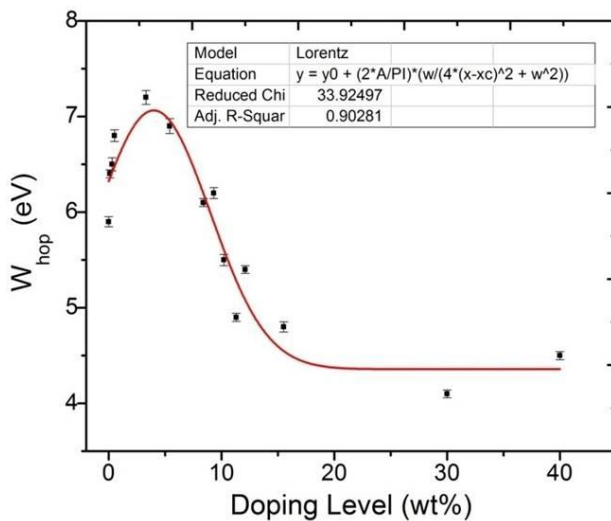


Figure 5 Variation of hopping energy (W_{hop}) with doping level of $CdCl_2$ in PVA-PVP blend (expressed in wt%).

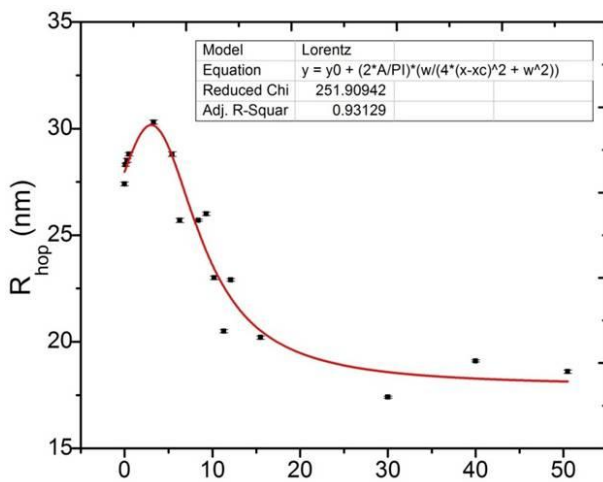


Figure 6 Variation of range of hopping (R_{hop}) with doping level (expressed in wt%) of $CdCl_2$ in PVA-PVP blend. The numbers shown in the X-axis represent the doping level (wt%).

In order to find the type of charge species contributing to DC conduction mechanism, determination of transference or transport number is essential. According to Wagner's polarization technique [47], transference number can be determined using discharge currents. The DC polarization technique is a simple, yet effective method for determining the transference number of ions and electrons [48]. Transference number measurements on un-doped and CdCl₂ doped PVA PVP blend films reveal that the charge carriers for DC electrical conductivity are mainly ions, although the transfer of electrons is also significant. See Figure 7, for the time evolution of DC electric current through the sample, under the influence of an applied (step) DC voltage/ potential difference of 1.1 volt across the sample.

$$t_{ele} = \frac{I_{ele}}{I_T} \quad (7)$$

In equation (7), I_{ele} is final current (I_f) due to electrons, and the total current, I_T , is initial current (I_i), that is current immediately after the step voltage is applied, which is due to migration of both ions and electrons as mobile charge carriers in the CdCl₂ doped PVA-PVP film. The symbols, t_{ele} and t_{ion} , represent the transference numbers for electrons and ions, respectively.

$$t_{ion} = 1 - t_{ele} \quad (8)$$

The estimated values of transference number of ions and electrons, for CdCl₂ doped PVA-PVP blend films, are listed in Table 2. The time evolution of DC electric current which has been observed over a time of 600 minutes, for an applied potential difference (voltage) of 1.1 volt, is shown in Figure 7. The data listed in Table 2 reveals that electrical conduction in case of CdCl₂ doped PVA-PVP blend films is due to both ions and electrons, but the major contribution is from ions. This implies that Cd²⁺ and Cl⁻ ions are also involved in carrying the ionic current in the doped polymeric blend, under the influence of applied potential difference.

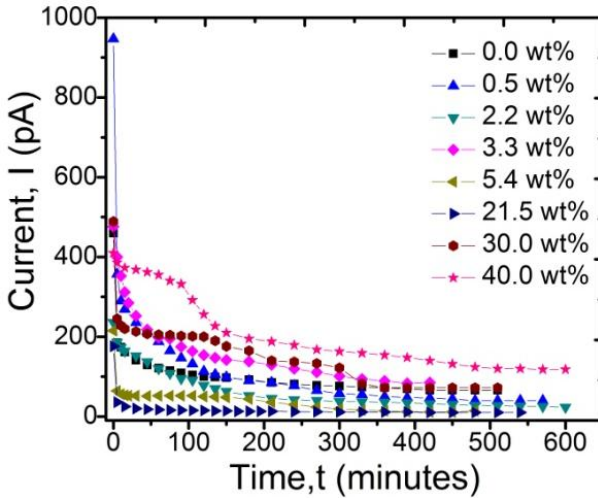


Figure 7 DC polarization current versus time at different concentration of CdCl₂ in PVA-PVP blend films. The plots shown here are for different doping levels (expressed in wt%) of CdCl₂ in PVA-PVP blend films.

DL (wt%)	t_{ele}	t_{ion}
0.0	0.143	0.857
0.5	0.092	0.908
2.2	0.097	0.903
3.3	0.174	0.826
5.4	0.051	0.949
15.5	0.114	0.885
21.5	0.057	0.943
30.0	0.147	0.853
40.0	0.200	0.800

Table 2 Transference number measurements reveal that the charge carriers for DC electrical conductivity are mainly ions, although the transfer of electrons is also significant. The symbols, t_{ele} and t_{ion} represent the transference numbers for electrons and ions, respectively.

4. Conclusion

PVA-PVP polymeric blend samples show a significant variation of DC electrical conductivity, on addition of CdCl₂ as the dopant. The values of activation energy (for samples doped to different levels) were obtained using Arrhenius equation and the three dimensional VRH model. Mott’s parameters were determined for pure and

CdCl₂ doped PVA-PVP blend films. Three different regions of polymeric microstructure can be gauged from the variation of DC electrical conductivity with temperature. They are correlated with formation of nano-structures, aggregation and phase separation of CdCl₂ in PVA-PVP blend. The time evolution of DC current (DC polarization current) reveals that charge transport is due to both ions and electrons, although ions are the dominant charge carriers in CdCl₂ doped PVA-PVP blend films.

Acknowledgements

Author B. M. Baraker thanks the Karnatak University, Dharwad (KUD), for providing UPE fellowship.

References

- [1] A. M. Stephan, "Review on gel polymer electrolytes for lithium batteries," *Eur. Polym. J.*, vol. 42, no. 1, pp. 21–42, 2006.
- [2] Y. Wang, K. S. Chen, J. Mishler, S. C. Cho, and X. C. Adroher, "A review of polymer electrolyte membrane fuel cells: technology, applications, and needs on fundamental research," *Appl. Energy*, vol. 88, no. 4, pp. 981–1007, 2011.
- [3] M. Hussain, Y. H. Ko, and Y. H. Choa, "Significant enhancement of mechanical and thermal properties of thermoplastic polyester elastomer by polymer blending and nanoinclusion," *J. Nanomater.*, vol. 2016, p. 69, 2016.
- [4] S. Thomas, R. Shanks, and S. Chandran, *Nanostructured polymer blends*. William Andrew, 2013.
- [5] A. G. Skirtach *et al.*, "The role of metal nanoparticles in remote release of encapsulated materials," *Nano Lett.*, vol. 5, no. 7, pp. 1371–1377, 2005.
- [6] X. Wang *et al.*, "Polymer-encapsulated gold-nanoparticle dimers: facile preparation and catalytical application in guided growth of dimeric ZnO-nanowires," *Nano Lett.*, vol. 8, no. 9, pp. 2643–2647, 2008.
- [7] M. Krumova, D. Lopez, R. Benavente, C. Mijangos, and J. M. Perena, "Effect of crosslinking on the mechanical and thermal properties of poly (vinyl alcohol)," *Polymer (Guildf.)*, vol. 41, no. 26, pp. 9265–9272, 2000.
- [8] G. Paradossi, F. Cavalieri, E. Chiessi, C. Spagnoli, and M. K. Cowman, "Poly (vinyl alcohol) as versatile biomaterial for potential biomedical applications," *J. Mater. Sci. Mater. Med.*, vol. 14, no. 8, pp. 687–691, 2003.

- [9] B. Lobo, M. R. Ranganath, T. S. G. R. Chandran, G. V. Rao, V. Ravindrachary, and S. Gopal, "Iodine-doped polyvinylalcohol using positron annihilation spectroscopy," *Phys. Rev. B*, vol. 59, no. 21, p. 13693, 1999.
- [10] M. Abdelaziz and M. M. Ghannam, "Influence of titanium chloride addition on the optical and dielectric properties of PVA films," *Phys. B Condens. Matter*, vol. 405, no. 3, pp. 958–964, 2010.
- [11] R. F. Bhajantri, V. Ravindrachary, A. Harisha, C. Ranganathaiah, and G. N. Kumaraswamy, "Effect of barium chloride doping on PVA microstructure: positron annihilation study," *Appl. Phys. A*, vol. 87, no. 4, pp. 797–805, 2007.
- [12] S. Kramadhathi and K. Thyagarajan, "Optical Properties of Pure and Doped (Kno₃ & Mgcl₂) Polyvinyl Alcohol Polymer Thin Films," *Int. J. Eng. Res. Dev.*, vol. 6, no. 8, pp. 15–18, 2013.
- [13] O. G. Abdullah, S. A. Hussien, A. Alani, M. Mehtap Demirel, O. G. Abdullah, and B. K. Aziz, "Electrical characterization of polyvinyl alcohol films doped with sodium iodide," *Asian Trans Sci Technol*, vol. 1, pp. 1–4, 2011.
- [14] F. Haaf, A. Sanner, and F. Straub, "Polymers of N-Vinylpyrrolidone: Synthesis, Characterization and Uses," *Polym J*, vol. 17, no. 1, pp. 143–152, Jan. 1985.
- [15] M. Ravi, Y. Pavani, K. K. Kumar, S. Bhavani, A. K. Sharma, and V. V. R. N. Rao, "Studies on electrical and dielectric properties of PVP: KBrO₄ complexed polymer electrolyte films," *Mater. Chem. Phys.*, vol. 130, no. 1, pp. 442–448, 2011.
- [16] J. Y. Chang *et al.*, *Biopolymers · PVA Hydrogels Anionic Polymerisation Nanocomposites*, vol. 153. Springer Science & Business Media, 2000.
- [17] J. Lu, Q. Nguyen, J. Zhou, and Z. Ping, "Poly (vinyl alcohol)/poly (vinyl pyrrolidone) interpenetrating polymer network: Synthesis and pervaporation properties," *J. Appl. Polym. Sci.*, vol. 89, no. 10, pp. 2808–2814, 2003.
- [18] S. A. Chen and H. T. Lee, "Structure and properties of poly (acrylic acid)-doped polyaniline," *Macromolecules*, vol. 28, no. 8, pp. 2858–2866, 1995.
- [19] N. Rajeswari, S. Selvasekarapandian, S. Karthikeyan, C. Sanjeeviraja, Y. Iwai, and J. Kawamura, "Structural, vibrational, thermal, and electrical properties of PVA/PVP biodegradable polymer blend electrolyte with CH₃COONH₄," *Ionics (Kiel)*, vol. 8, no. 19, pp. 1105–1113, 2013.
- [20] E. M. Abdelrazek, I. S. Elashmawi, A. El-Khodary, and A. Yassin, "Structural, optical, thermal and electrical studies on PVA/PVP blends filled with lithium bromide," *Curr. Appl. Phys.*, vol. 10, no. 2, pp. 607–613, 2010.

- [21] I. S. Elashmawi and H. E. A. Baieth, "Spectroscopic studies of hydroxyapatite in PVP/PVA polymeric matrix as biomaterial," *Curr. Appl. Phys.*, vol. 12, no. 1, pp. 141-146, 2012.
- [22] H. M. Ragab, "Spectroscopic investigations and electrical properties of PVA/PVP blend filled with different concentrations of nickel chloride," *Phys. B Condens. Matter*, vol. 406, no. 20, pp. 3759-3767, 2011.
- [23] M. Pandey, G. M. Joshi, K. Deshmukh, and J. Ahmad, "Impedance spectroscopy and conductivity studies of CdCl₂ doped polymer electrolyte," *J Adv Mater Lett*, vol. 6, no. 2, pp. 165-171, 2015.
- [24] B. M. Baraker, P. B. Hammannavar, and B. Lobo, "Optical, electrical, thermal properties of cadmium chloride doped PVA-PVP blend," in *AIP Conference Proceedings*, 2015, vol. 1665, no. 1, p. 70037.
- [25] B. M. Baraker and B. Lobo, "Dispersion parameters of cadmium chloride doped PVA-PVP blend films," *J. Polym. Res.*, vol. 5, no. 24, pp. 1-10, 2017.
- [26] B. M. Baraker and B. Lobo, "Spectroscopic Analysis of CdCl₂ doped PVA-PVP Blend Films," *Can. J. Phys.*, 2017.
- [27] B. M. Baraker and B. Lobo, "Experimental study of PVA-PVP blend films doped with cadmium chloride monohydrate," *Indian J. Pure Appl. Phys.*, vol. 54, no. 10, pp. 634-640, 2016.
- [28] T. Pradeep, *Nano: the essentials*. Tata McGraw-Hill Education, 2007.
- [29] K. K. Kumar, M. Ravi, Y. Pavani, S. Bhavani, A. K. Sharma, and V. V. R. N. Rao, "Investigations on the effect of complexation of NaF salt with polymer blend (PEO/PVP) electrolytes on ionic conductivity and optical energy band gaps," *Phys. B Condens. Matter*, vol. 406, no. 9, pp. 1706-1712, 2011.
- [30] R. M. Hodge, G. H. Edward, and G. P. Simon, "Water absorption and states of water in semicrystalline poly (vinyl alcohol) films," *Polymer (Guildf)*, vol. 37, no. 8, pp. 1371-1376, 1996.
- [31] A. Arsenlis and D. M. Parks, "Crystallographic aspects of geometrically-necessary and statistically-stored dislocation density," *Acta Mater.*, vol. 47, no. 5, pp. 1597-1611, 1999.
- [32] G. Krishna Bama, P. Indra Devi, and K. Ramachandran, "Structural and thermal properties of PVDF/PVA blends," *J. Mater. Sci.*, vol. 44, no. 5, pp. 1302-1307, 2009.
- [33] J. D. Hanawalt, H. W. Rinn, and L. K. Frevel, "Chemical analysis by X-ray diffraction," *Ind. Eng. Chem. Anal. Ed.*, vol. 10, no. 9, pp. 457-512, 1938.
- [34] H. E. Swanson, R.K. Fuyat, Natl. Bur. Stand.(U.S), Circ. 539 (III), 10, (1954)
- [35] C. K. Chiang *et al.*, "Electrical Conductivity in Doped Polyacetylene," *Phys. Rev. Lett.*, vol. 40, no. 22, p. 1472, 1978.

- [36] C. C. Ku and R. Liepins, *Electrical properties of polymers*. MacMillan Publishing Company, 1993.
- [37] P. Sharma, D. K. Kanchan, N. Gondaliya, M. Jayswal, and P. Joge, "Influence of nano filler on conductivity in PEO-PMMA-AgNO₃ polymer blend," 2013.
- [38] J. B. González-Campos *et al.*, "Molecular dynamics analysis of PVA-AgNP composites by dielectric spectroscopy," *J. Nanomater.*, vol. 2012, p. 10, 2012.
- [39] S. Mahendia, A. K. Tomar, and S. Kumar, "Electrical conductivity and dielectric spectroscopic studies of PVA-Ag nanocomposite films," *J. Alloys Compd.*, vol. 508, no. 2, pp. 406–411, 2010.
- [40] F. Lux, "Models proposed to explain the electrical conductivity of mixtures made of conductive and insulating materials," *J. Mater. Sci.*, vol. 28, no. 2, pp. 285–301, 1993.
- [41] P. B. Bhargav, B. A. Sarada, A. K. Sharma, and V. Rao, "Electrical conduction and dielectric relaxation phenomena of PVA based polymer electrolyte films," *J. Macromol. Sci. Part A*, vol. 47, no. 2, pp. 131–137, 2009.
- [42] A. Yildiz, S. B. Lisesivdin, M. Kasap, and D. Mardare, "Electrical properties of TiO₂ thin films," *J. Non. Cryst. Solids*, vol. 354, no. 45, pp. 4944–4947, 2008.
- [43] K. P. Nazeer, M. Thamilselvan, D. Mangalaraj, S. K. Narayandass and J. Yi, *J. Polym. Res.* 13(1), 17 (2006).
- [44] N. F. Mott and E. A. Davis. *Electronic processes in Non-crystalline Materials*. 2nd ed. Oxford University Press. 1979. ISBN: 9780199645336
- [45] V. Ambegaokar, B. I. Halperin, and J. S. Langer, "Hopping conductivity in disordered systems," *Phys. Rev. B*, vol. 4, no. 8, p. 2612, 1971.
- [46] R. P. Sharma, A. K. Shukla, A. K. Kapoor, R. Srivastava, and P. C. Mathur, "Hopping conduction in polycrystalline semiconductors," *J. Appl. Phys.*, vol. 57, no. 6, pp. 2026–2029, 1985.
- [47] J. B. Wagner and C. Wagner, "Electrical conductivity measurements on cuprous halides," *J. Chem. Phys.*, vol. 26, no. 6, pp. 1597–1601, 1957.
- [48] R. C. Agrawal, "dc Polarisation: An experimental tool in the study of ionic conductors," *Indian J. Pure Appl. Phys.*, vol. 37, no. 4, pp. 294, 1999.